

## Evidence for electron-hole pairing in graphene-GaAs double layers

A. GAMUCCI<sup>(\*)</sup>

*National Enterprise for Nanoscience and Nanotechnology (NEST), Istituto Nanoscienze-C Consiglio Nazionale delle Ricerche and Scuola Normale Superiore, I-56126 Pisa, Italy*

received 26 February 2015

**Summary.** — Spatially separated two-dimensional systems of electrons and holes are predicted to condense below a critical temperature into a neutral superfluid state of electron-hole pairs, called “exciton condensate”. Here evidence of this scenario is presented in systems of massless Dirac holes in a graphene flake in close proximity of electrons hosted in a gallium arsenide quantum well. A logarithmic enhancement of Coulomb drag at zero magnetic field and temperatures below 5 K, which we attribute to pairing fluctuations extending above the temperature for exciton condensation, has been found experimentally. Our Dirac-Schrödinger hybrid system offers a new benchmark to study superfluidity in reduced spatial dimensions.

PACS 72.80.Vp – Electronic transport in graphene.  
PACS 71.35.-y – Excitons and related phenomena.

### 1. – Introduction

The physics of excitons in solid state systems has been investigated in different experiments in the last decades [1, 2]. Bose-Einstein condensation of electron-hole pairs has been studied with notable results [3], while condensation of optically excited exciton cold gases has been reported [4]. For what concerns double quantum wells systems in GaAs/AlGaAs heterostructures, a series of transport anomalies can occur in quantum Hall electron and hole fluids [5].

Recently new focus is put on interlayer excitons, *i.e.* electron-hole pairs forming from electrons and holes belonging to different layers, under the push of theoretical predictions of spontaneous coherence and superfluidity at non-cryogenic temperatures and relatively weak magnetic fields [6-8]. Permanent excitons showing spontaneous coherence and superfluidity effects are thus studied at non-extreme physical conditions while a fundamental interest is raised in understanding the occurrence of these phenomena in nature.

---

<sup>(\*)</sup> *Present address:* Istituto Italiano di Tecnologia, Graphene Labs - I-16163, Genova, Italy.

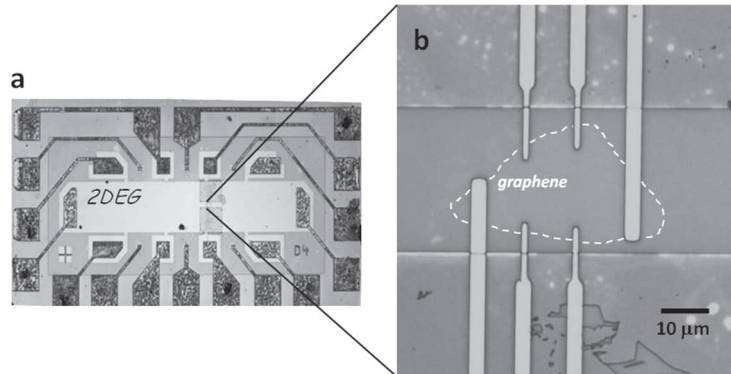


Fig. 1. – a) Optical microscope image of the device showing the Hall bar mesa with Ohmic contacts and the etched channel in correspondence of the graphene flake. b) Optical microscope magnification of the contacted graphene flake on the etched 2D GaAs channel. The dashed line denotes the boundaries of the graphene. The graphene flake becomes visible in green light after the sample has been coated with PMMA polymer.

In this paper heterostructures comprising a single-layer graphene carrying a fluid of massless chiral carriers [9], and a quantum well created in GaAs/AlGaAs 31.5 nm below the surface, hosting a high-mobility two-dimensional electron gas (2DEG) are investigated. These represent a new class of double-layer devices composed of spatially separated electron and hole fluids. We find that the Coulomb drag resistivity significantly increases for temperatures below 5–10 K, following a logarithmic law. This anomalous behavior is a signature of the onset of strong interlayer correlations, compatible with the formation of a condensate of permanent excitons. Artificially induced strongly correlated electron-hole states are a benchmark for the realization of coherent circuits with minimal dissipation [10, 11] and nanodevices [12, 13].

## 2. – Fabrication and characterization of the device

The investigated device consists of a Dirac-Schrödinger hybrid electron system made up of a monolayer graphene flake transferred on top of a GaAs/AlGaAs heterostructure hosting a high-mobility shallow 2DEG. A monolayer graphene flake is mechanically exfoliated onto SiO<sub>2</sub>/Si, and then transferred onto the GaAs sample and placed over the Hall bar. Raman spectroscopy and atomic force microscopy ensure that the flake is a monolayer and that the transfer process did not damage it. A Hall bar is fabricated on the 2DEG and Ohmic contacts were fabricated on the graphene. In order to make sure that current in the 2DEG flows only in the region below the graphene, a narrow channel of  $\sim 50 \mu\text{m}$  width is defined in the Hall bar just below the graphene flake by means of electron beam lithography and wet etching (see fig. 1).

To fully characterize our sample, we first performed magneto-transport measurements at 4 K in the two separated layers, as reported in fig. 2. In the 2DEG the electron density is found to be  $1.2 \cdot 10^{11} \text{ cm}^{-2}$  from low-field classical Hall effect and the mobility is  $13000 \text{ cm}^2/\text{Vs}$  at 4 K; at 45 K, the density decreases to  $4.0 \cdot 10^{10} \text{ cm}^{-2}$  and the mobility to  $8700 \text{ cm}^2/\text{Vs}$ . The 2DEG is induced in the quantum well by shining light by an infrared LED before the measurements. When the 2DEG is not induced (fig. 2(c), (d)), we found

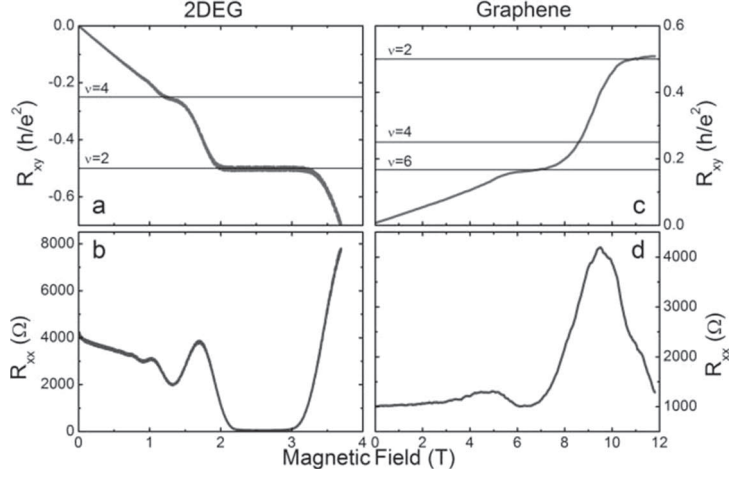


Fig. 2. – a) Hall resistance of 2DEG. Horizontal lines indicate the resistance values of integer quantum Hall effect plateaus ( $R_{xy} = (1/\nu) \cdot (h/e^2)$  at plateau position). b) Longitudinal resistance of 2DEG. c) d) Hall and longitudinal resistances for graphene. The Hall measurements are taken in the two layers with the same topological configuration of electrical connections: Hall resistance is positive for holes and negative for electrons.

that carriers in graphene are holes, as evident from fig. 2(c) where the sign of Hall resistance  $R_{xy}$  is opposite with respect to the 2DEG case (fig. 2(a)). At 4K the hole density is  $9.9 \cdot 10^{11} \text{ cm}^{-2}$  and the mobility is  $4100 \text{ cm}^2/\text{Vs}$ ; at 45K the values are  $6.7 \cdot 10^{11} \text{ cm}^{-2}$  and  $2400 \text{ cm}^2/\text{Vs}$  for density and mobility, respectively. When the 2DEG is induced, graphene transport properties are markedly affected. In particular, we find that at 4K the hole density is  $6.7 \cdot 10^{11} \text{ cm}^{-2}$  and the mobility is reduced to  $2100 \text{ cm}^2/\text{Vs}$ . We can explain this behavior considering that charged impurities are left in the heterostructure when the 2DEG is induced, resulting in an enhanced scattering of graphene carriers which reduces the mobility. In fig. 2 we can observe the Quantum Hall Effect in both 2DEG and graphene, confirming the quality of the two layers. In the 2DEG (fig. 2(a)) we find plateaus at  $e^2/2h$  and  $e^2/4h$ , corresponding to the first two spin degenerate Landau levels. Corresponding to the plateaus, minima are found in the longitudinal resistance fig. 2(b). In graphene fig. 2(c) we found, as expected, a plateau at  $e^2/2h$  and one at  $e^2/6h$ , corresponding to Dirac fermions with spin and valley degeneracy.

### 3. – Coulomb drag results

In a Coulomb drag experiment [14-16] current is sent in one of the two layers (the *active* layer) and the induced voltage drop at the edges of the other layer (the *passive* layer) is measured with a voltmeter. The passive layer can be assumed to be an open circuit (no current can flow in it), so that the drive current  $I_{\text{drive}}$  drags carriers in the passive layer, which accumulate at the ends of the layer, building up the voltage drop. Correlations between the 2DEG in the GaAs quantum well and the hole fluid [9] in graphene are studied by measuring the temperature dependence of the Coulomb drag resistance  $R_D$ . The quantity  $R_D$  is defined as the ratio  $V_{\text{drag}}/I_{\text{drive}}$  and is determined by the rate of momentum transfer between quasiparticles in the two layers [16].

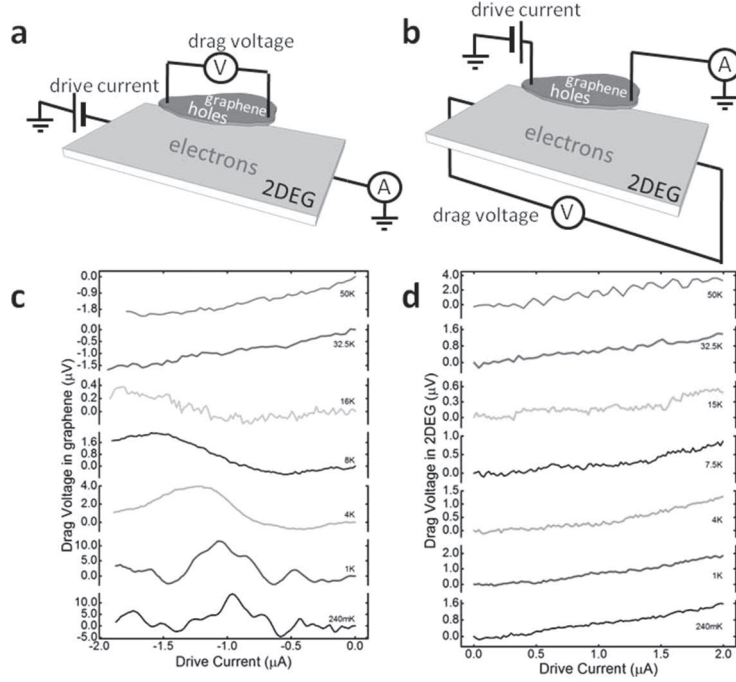


Fig. 3. – a) b) Electrical connections for the experiment on Coulomb drag in graphene and in the 2DEG. c) Drag voltage measured in graphene as a function of negative driving current flowing in the 2DEG layer for different temperatures. d) Drag voltage measured in the 2DEG as a function of positive driving current flowing in graphene for different temperatures.

The schematics for the Coulomb drag experiments are shown in fig. 3(a), (b). The measurements are carried out at different temperatures in the range 240 mK–50 K in a  $^3\text{He}$  cryostat, injecting a DC drive current  $I_{\text{drive}}$  in one layer and measuring the drag voltage  $V_{\text{drag}}$  in the other. The drive current is always monitored in our set-up. Several  $V_{\text{drag}}-I_{\text{drive}}$  curves are acquired for each temperature, and then averaged. We employed the DC configuration to avoid capacitive coupling between the layers. In a drag measurement it is important to ensure that no leakage current is flowing from one layer to the other. In our case, we found that the interlayer resistance is of the order of  $1\text{ G}\Omega$  at every temperature, much larger than the resistance of the layers (of the order of a few  $\text{k}\Omega$ ).

The measurement of drag resistance induced in graphene by driving current in the 2DEG has been carried out applying a negative current in the latter, from 0 to  $-2\text{ }\mu\text{A}$ . In this way, we prevented the carriers in the 2DEG from depleting as a consequence of gating effect induced by the graphene. The measured drag voltage at different temperatures is shown in fig. 3(c), (d) for drag in graphene and in 2DEG, respectively. When the drag in graphene is considered, at the lowest temperatures, the induced voltage presents a series of oscillations which can be linked to mesoscopic fluctuations occurring in graphene at low  $T$ . These fluctuations start vanishing from temperatures higher than 16 K, at which the drag voltage becomes linear. In the case of drag induced in the 2DEG by a current flowing in the graphene, the gating effect and consequent carrier depletion has been avoided applying a positive sign current (0 to  $+2\text{ }\mu\text{A}$ ) in the graphene flake. As expected, no fluctuations arise in this case at any temperature and a linear  $V_{\text{drag}}-I_{\text{drive}}$  relation is found in the whole temperature range. Values of drag resistance for the 2DEG have thus been extracted for the temperature range 30 K–50 K and they are shown in fig. 4(a), (b).

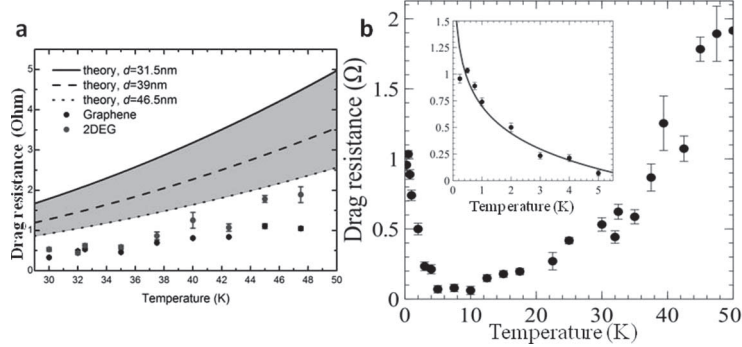


Fig. 4. – a) Drag resistances calculated for graphene and 2DEG for the temperature range 30 K–50 K. The shaded region corresponds to the theoretical prediction for a hybrid Dirac/Schrödinger SLG/2DEG double layer within a Boltzmann-transport theory. b) Drag resistance obtained in the 2DEG (passive layer) *vs.* temperature. The inset is a zoom of  $R_D$  in the low- $T$  limit. The red solid line is a fit based on the equation reported in eq. (1).

Figure 4(a) shows the drag resistance measured when the passive layer is alternatively the 2DEG (brighter points) or graphene (black points), for  $30 \text{ K} \leq T \leq 50 \text{ K}$ , with the other layer used as the drive or passive layer. The result of theoretical calculations of the  $T$  dependence of  $R_D$  in a hybrid Dirac/Schrödinger SLG/2DEG double layer within a Boltzmann-transport theory in the Fermi-liquid regime is also shown [18,19]. The experimental results in this  $T$  range match the canonical Fermi-liquid prediction [14,17-19]. The measured data are however slightly reduced with respect to the calculations. This effect has already been reported for Coulomb drag measurements in graphene-graphene systems hosted in hexagonal boron nitride [7]. Figure 4(a) shows that the Onsager reciprocity relation [20,21], *i.e.* the equivalence of measured resistance values when drive and passive layer are interchanged, is satisfied just in the  $30 \text{ K} \leq T \leq 40 \text{ K}$  range, while a violation of the Onsager relation takes place for  $T > 40 \text{ K}$ . The experimental data thus show for  $T > 40 \text{ K}$  a mismatch when the active and passive layers are interchanged. This discrepancy can be ascribed to the effect of a leak interlayer current, which can bring additional contributions sensitive to the exchange of active and passive layers [1].

Focusing on the Coulomb drag measurements in the 2DEG, with the graphene acting as active layer, it can be noted that in the low-temperature regime (see the inset of fig. 4(b)), the drag resistance in the 2DEG has an anomalous increase below 10 K, departing from the Fermi-liquid typical  $T^2$  dependence. There is in fact a clear upturn at a temperature around 5 K, below which the resistance increases by more than one order of magnitude. Data can be fitted in this region with a curve of the form [22,23]

$$(1) \quad R_D(T) = R_0 + A \log \left( \frac{T_c}{T - T_c} \right),$$

where  $R_0$  and  $A$  are two fitting parameters and  $T_c$  is the mean-field critical temperature of a low- $T$  phase transition.

The logarithmic upturn of the drag resistance in 2DEG fitted with the above equation has been theoretically predicted [22,23] on the basis of a Boltzmann transport theory for electron-hole double layers. In this model the scattering amplitude is calculated in a ladder approximation [24]. Similar results were obtained with a Kubo-formula

approach [25]. The obtained enhancement can thus be attributed to fluctuations in pairing of electron-hole couples that extends above  $T_c$  for a phase transition into an excitonic condensate [22, 25].

#### 4. – Conclusion

Exciton condensation is studied in a large number of experiments involving several solid-state systems. Those systems range from microcavities in semiconductor showing exciton-polaritons with ultrashort lifetimes [3] to indirect excitons in asymmetric semiconductor double quantum wells [4]. Upturn of Coulomb drag resistivity was instead evidenced in electron-hole doped GaAs/AlGaAs double quantum wells [26, 27]. The difficulty of creating a systems with electron and hole layers in the same semiconductor heterostructure relies however in a huge fabrication effort, while the coupling of two graphene flakes makes the observation of Coulomb drag anomalies at low temperature impossible due to the rise of mesoscopic fluctuations inhibiting the measurement of a linear  $V_{\text{drag}}-I_{\text{drive}}$  relation. The presented vertical heterostructures bypass these problems by joining the advantages of two different 2D electron systems. 2D electron and hole fluids are combined in the presented hybrid heterostructures with state-of-the-art nanofabrication processing. These represent a new class of vertical heterostructure devices with large flexibility in the design of characteristic features like band dispersions, doping, and electron-hole coupling, in which excitonic effects can be studied with ease.

Inter-layer excitons can represent the building blocks for coherent interconnections between electronic signal processing and optical communications [10, 11] as well for a variety of applications like analog-to-digital converters [12].

\* \* \*

Thanks are due to D. SPIRITO, M. CARREGA, B. KARMAKAR, A. LOMBARDO, M. BRUNA, L. N. PFEIFFER, K. W. WEST, A. C. FERRARI, M. POLINI and V. PELLEGRINI for the implementation and interpretation of the experiments, and to R. DUINE, R. FAZIO, A. HAMILTON, M. KATSNELSON, A. MACDONALD, D. NEILSON, K. NOVOSELOV, A. PERALI, A. PINCZUK and G. VIGNALE for useful discussions. We acknowledge funding from EU Graphene Flagship (contract no. CNECT-ICT-604391), EC ITN project “INDEX” Grant No. FP7-2011-289968, the Italian Ministry of Education, University, and Research (MIUR) through the program “FIRB - Futuro in Ricerca 2010” Grant No. RBFR10M5BT (“PLASMOGRAPH”), ERC grants NANOPOTS, Hetero2D, a Royal Society Wolfson Research Merit Award, EU projects GENIUS, CARERAMM, RODIN, EPSRC grants EP/K01711X/1, and EP/K017144/1.

#### REFERENCES

- [1] GAMUCCI A., SPIRITO D., CARREGA M., KARMAKAR B., LOMBARDO A., BRUNA M., PFEIFFER L. N., WEST K. W., FERRARI A. C., POLINI M. and PELLEGRINI V., *Nat. Commun.*, **5** (2014) 5824, doi:10.1038/ncomms6824 (2014).
- [2] For a recent review see, *e.g.*, RONTANI M. and SHAM L. J., *Coherent exciton transport in semiconductors*, in *Novel Superfluids*, Vol. **2**, edited by BENNEMANN K. H. and KETTERSON J. B. *International Series of Monographs on Physics*, no. 157 (Oxford University Press) 2014.
- [3] KASPRZAK J., RICHARD M., KUNDERMANN S., BAAS A., JEAMBRUN P., KEELING J. M. J., MARCHETTI F. M., SZYMAŃSKA M. H., ANDRÉ R., STAEHLI J. L., SAVONA V., LITTLEWOOD P. B., DEVEAUD B. and DANG LE SI, *Nature*, **443** (2006) 409.

- [4] HIGH A. A., LEONARD J. R., HAMMACK A. T., FOGLER M. M., BUTOV L. V., KAVOKIN A. V., CAMPMAN K. L. and GOSSARD A. C., *Nature*, **483** (2012) 584.
- [5] NANDI D., FINCK A. D. K., EISENSTEIN J. P., PFEIFFER L. N. and WEST K. W., *Nature*, **488** (2012) 481.
- [6] KIM S., JO I., NAH J., YAO Z., BANERJEE S. K. and TUTUC E., *Phys. Rev. B*, **83** (2011) 161401(R).
- [7] GORBACHEV R. V., GEIM A. K., KATSNELSON M. I., NOVOSELOV K. S., TUDOROVSKIY T., GRIGORIEVA I. V., MACDONALD A. H., MOROZOV S. V., WATANABE K., TANIGUCHI T. and PONOMARENKO L. A., *Nat. Phys.*, **8** (2012) 896.
- [8] KIM S. and TUTUC E., *Solid State Commun.*, **152** (2012) 1283.
- [9] GEIM A. K. and NOVOSELOV K. S., *Nat. Mater.*, **6** (2007) 183.
- [10] HIGH A. A., NOVITSKAYA E. E., BUTOV L. V. and GOSSARD A. C., *Science*, **321** (2008) 229.
- [11] BALLARINI D., DE GIORGI M., CANCELLIERI E., HOUDRÉ R., GIACOBINO E., CINGOLANI R., BRAMATI A., GIGLI G. and SANVITTO D., *Nat. Commun.*, **4** (2013) 1778.
- [12] DOLCINI F., RAINIS D., TADDEI F., POLINI M., FAZIO R. and MACDONALD A. H., *Phys. Rev. Lett.*, **104** (2010) 027004.
- [13] PEOTTA S., GIBERTINI M., DOLCINI F., TADDEI F., POLINI M., IOFFE L. B., FAZIO R. and MACDONALD A. H., *Phys. Rev. B*, **84** (2011) 184528.
- [14] GRAMILA T. J., EISENSTEIN J. P., MACDONALD A. H., PFEIFFER L. N. and WEST K. W., *Phys. Rev. Lett.*, **66** (1991) 1216.
- [15] SIVAN U., SOLOMON P. M. and SHTRIKMAN H., *Phys. Rev. Lett.*, **68** (1992) 1196.
- [16] ROJO A. G., *J. Phys.: Condens. Matter*, **11** (1999) R31.
- [17] KAMENEV A. and OREG Y., *Phys. Rev. B*, **52** (1995) 7516.
- [18] CARREGA M., TUDOROVSKIY T., PRINCIPI A., KATSNELSON M. I. and POLINI M., *New J. Phys.*, **14** (2012) 063033.
- [19] PRINCIPI A., CARREGA M., ASGARI R., PELLEGRINI V. and POLINI M., *Phys. Rev. B*, **86** (2012) 085421.
- [20] ONSAGER L. I., *Phys. Rev.*, **37** (1931) 405.
- [21] ONSAGER L., *Phys. Rev.*, **38** (1931) 2265.
- [22] MINK M. P., STOOF H. T. C., DUINE R. A., POLINI M. and VIGNALE G., *Phys. Rev. Lett.*, **108** (2012) 186402.
- [23] MINK M. P., STOOF H. T. C., DUINE R. A., POLINI M. and VIGNALE G., *Phys. Rev. B*, **88** (2013) 235311.
- [24] LARKIN A. and VARLAMOV A., *Theory of Fluctuations in Superconductors* (Clarendon Press, Oxford) 2004.
- [25] HU B. Y.-K., *Phys. Rev. Lett.*, **85** (2000) 820.
- [26] CROXALL A. F., DAS GUPTA K., NICOLL C. A., THANGARAJ M., BEERE H. E., FARRER I., RITCHIE D. A. and PEPPER M., *Phys. Rev. Lett.*, **101** (2008) 246801.
- [27] SEAMONS J. A., MORATH C. P., RENO J. L. and LILLY M. P., *Phys. Rev. Lett.*, **102** (2009) 026804.